
PHYSICAL PROPERTIES
OF CRYSTALS

Peculiarities of the Dielectric Spectra of Triglycine Sulfate Crystals with a Profile Distribution of Chromium

E. S. Ivanova^{a,*}, G. I. Ovchinnikova^b, A. P. Ereemeev^{a,b}, V. V. Grebenev^a,
N. V. Belugina^a, and A. L. Tolstikhina^a

^a *Shubnikov Institute of Crystallography, Federal Scientific Research Centre “Crystallography and Photonics,”
Russian Academy of Sciences, Moscow, 119333 Russia*

^b *Faculty of Physics, Moscow State University, Moscow, Russia*

*e-mail: ivanova.el.ser@gmail.com

Received March 15, 2019; revised April 10, 2019; accepted April 12, 2019

Abstract—The temperature evolution of the dielectric spectra of TGS–TGS + Cr crystals (TGS stands for triglycine sulfate) with a periodic distribution of chromium impurity (Cr^{3+}) has been studied in comparison with nominally pure TGS crystals in the frequency range from 10 to 10^7 Hz upon heating and cooling. It is shown that impurity crystals are characterized by the absence of dielectric dispersion in both measurement modes. An approach is proposed to explain the peculiarities of the dielectric dispersion of crystals with a periodic distribution of chromium impurity from the standpoint of mobile activity of certain elements of the TGS crystal structure.

DOI: 10.1134/S1063774519050080

INTRODUCTION

Triglycine sulfate (TGS) is a well-known ferroelectric, which, starting from instant of its discovery [1], has been widely used in industry [2, 3]. Ferroelectrics with artificially introduced impurities, whose chemical nature determines to a great extent the most important electrical properties of these crystals, are used in many practical applications in radio electronics. Since the properties of ferroelectrics are structure-sensitive, the introduction of particular defects is a practically approved way to optimize their characteristics.

A systematically inhomogeneous introduction of impurities, which expands the range of existence of the ferroelectric phase and stabilizes the spontaneous polarization, provides additional possibilities for controlling the macroscopic properties of TGS [4]. Profile introduction of chromium impurity (Cr^{3+}) leads to the formation of a periodic growth structure in the crystal, which consists of alternating TGS + Cr and TGS stripes [5]. The dielectric properties of these stripe TGS–TGS + Cr crystals and the relaxation processes occurring in them have been investigated insufficiently, which motivated experimental studies in this field. Determination of the role of impurity in the molecular dynamics of crystal and the relaxation processes under electrical field and temperature effect is of particular interest.

The molecular dynamics is highly complicated in even nominally pure TGS crystals. Indeed, even now,

researchers discuss which of the dynamic processes initiates the phase transition [6–8] and what is the relationship between the macroscopic dielectric properties and structural transformations. Dielectric spectra are often analyzed when studying the structural phase transitions in ferroelectrics, including TGS crystals. Most researchers [9–16] explain the existence of dielectric dispersion in TGS crystals by the dynamics of domains and domain walls.

An important purpose of our study was to search for the possibilities of relating the mobile activity of certain structural elements of impurity TGS crystals with the permittivity dispersion in a wide frequency range. To solve this problem, we studied the temperature–frequency dynamics of TGS samples with a profile chromium distribution in comparison with nominally pure samples. It is known [17, 18] that Cr^{3+} ions are incorporated into the TGS structure in a certain way, which should manifest itself in the dynamics of dielectric spectra. To understand the relationship between the dielectric spectra and the processes of destruction and formation of ordered structure, measurements were performed upon heating and cooling in the temperature range of 23–60°C.

EXPERIMENTAL

TGS crystals (chemical formula $(\text{N}^+\text{H}_3\text{CH}_2\text{COOH})_2(\text{N}^+\text{H}_3\text{CH}_2\text{COO}^-) \cdot \text{SO}_4^{2-}$) were grown at the Shubnikov Institute of Crystallography

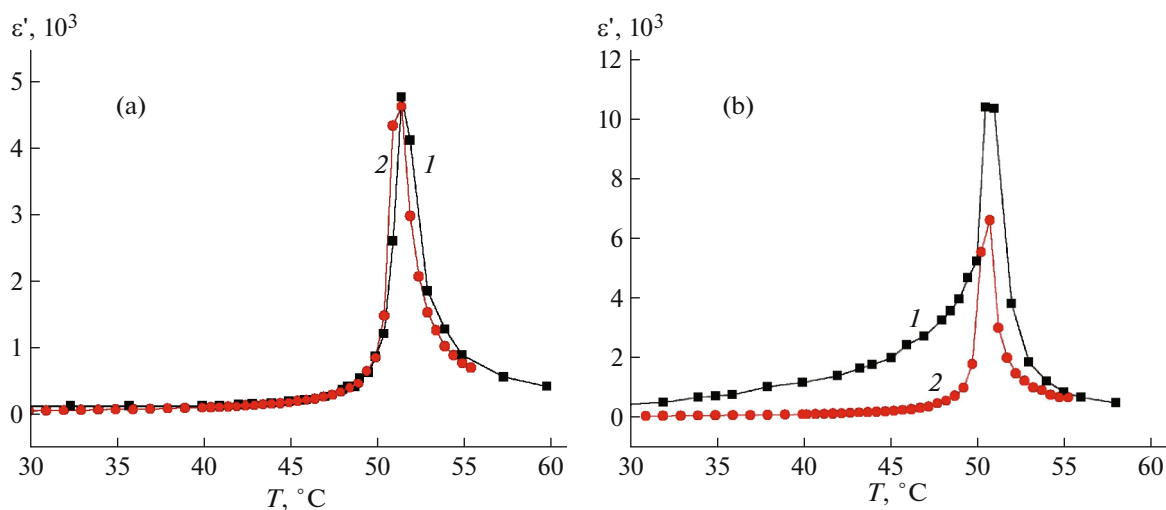


Fig. 1. Temperature dependences of the permittivity $\epsilon'(T)$ of (1) TGS and (2) TGS–TGS + Cr at a frequency of 1 kHz in the (a) heating and (b) cooling modes.

by isothermal evaporation at a temperature T lower than the phase-transition temperature T_C . Stripe TGS – TGS + Cr crystals were fabricated at the Institute of Technical Acoustics of the National Academy of Sciences of Belarus at $T = 31.4^\circ\text{C}$ by periodically growing up a seed in solutions of different compositions: pure TGS and TGS containing dopant Cr^{3+} ions with a content of 5–6 wt % [5]. The nominally pure and impurity bands emerging on the (010) surface were observed in an optical microscope; they had widths of 200 and 500 μm , respectively. Before carrying out dielectric measurements, crystals were annealed for 2 h at $T = 110^\circ\text{C}$.

The measurements of dielectric spectra, specifically, the temperature–frequency dependences of the real (ϵ') and imaginary (ϵ'') parts of complex permittivity, were performed in the frequency range from 10 to 10^7 Hz by impedance spectroscopy on a Novoterm-1200 system equipped with an impedance analyzer Alpha–AN. Spectra were recorded in the range of 23–60 $^\circ\text{C}$ with a step change in temperature and a high degree of stabilization at each point. The temperature settling time, especially near T_C , was 1 h or even longer. The samples were cut from a crystal in the form of plane-parallel plates $5 \times 5 \text{ mm}^2$ in size with a thickness of 1 mm, whose large faces were oriented perpendicular to the b (Y) axis. Silver paste was used as the electrode material.

RESULTS AND DISCUSSION

The investigations were performed according to the following scheme: first a crystal was heated from 23 to 60 $^\circ\text{C}$ with simultaneous measurement of dielectric spectra (heating mode); then the sample was kept at the maximum temperature for 1 h; and, finally, the

temperature was reduced with simultaneous measurement of spectra (cooling mode). The temperature dependences $\epsilon'(T)$, measured for the TGS and TGS–TGS + Cr samples at a frequency of 1 kHz upon (a) heating and (b) cooling, are presented in Fig. 1. One can see that the dielectric spectra of impurity crystals differ from the spectra of nominally pure TGS; these distinctions are most pronounced in the cooling mode (Fig. 1b). The presence of chromium in the TGS–TGS + Cr structure reduces by more than 40% the maximum $\epsilon'(T)$ value; note that the temperatures corresponding to the ϵ' maxima are equal within the measurement error (Fig. 1b, curves 1, 2). In addition, upon cooling, the range of anomalous rise in $\epsilon'(T)$ in the closest vicinity of the phase transition is significantly narrowed for the TGS–TGS + Cr samples as compared with TGS crystals. The anomalous rise in $\epsilon'(T)$ in the TGS–TGS + Cr crystal is observed in a relatively narrow temperature range (Fig. 1b, curve 2), whereas for the TGS crystal this range is much wider (Fig. 1b, curve 1). In the heating mode, no essential distinctions were revealed in the temperature dependences $\epsilon'(T)$ for the TGS–TGS + Cr crystal as compared with TGS. Concerning the two measurement modes, it should be noted that more significant changes in the character of the dependence $\epsilon'(T)$ occur for pure TGS. For the TGS–TGS + Cr sample, only absolute $\epsilon'(T)$ values in the vicinity of maximum increase upon cooling in comparison with the heating mode, whereas TGS is characterized, along with the increase in absolute $\epsilon'(T)$ values, by the expansion of the anomalous rise range near the $\epsilon'(T)$ maximum (Fig. 1).

Additional information about the specificity of the temperature dynamics of dielectric spectra of crystals can be derived from the frequency dependences of permittivity, measured at several (if possible, identi-

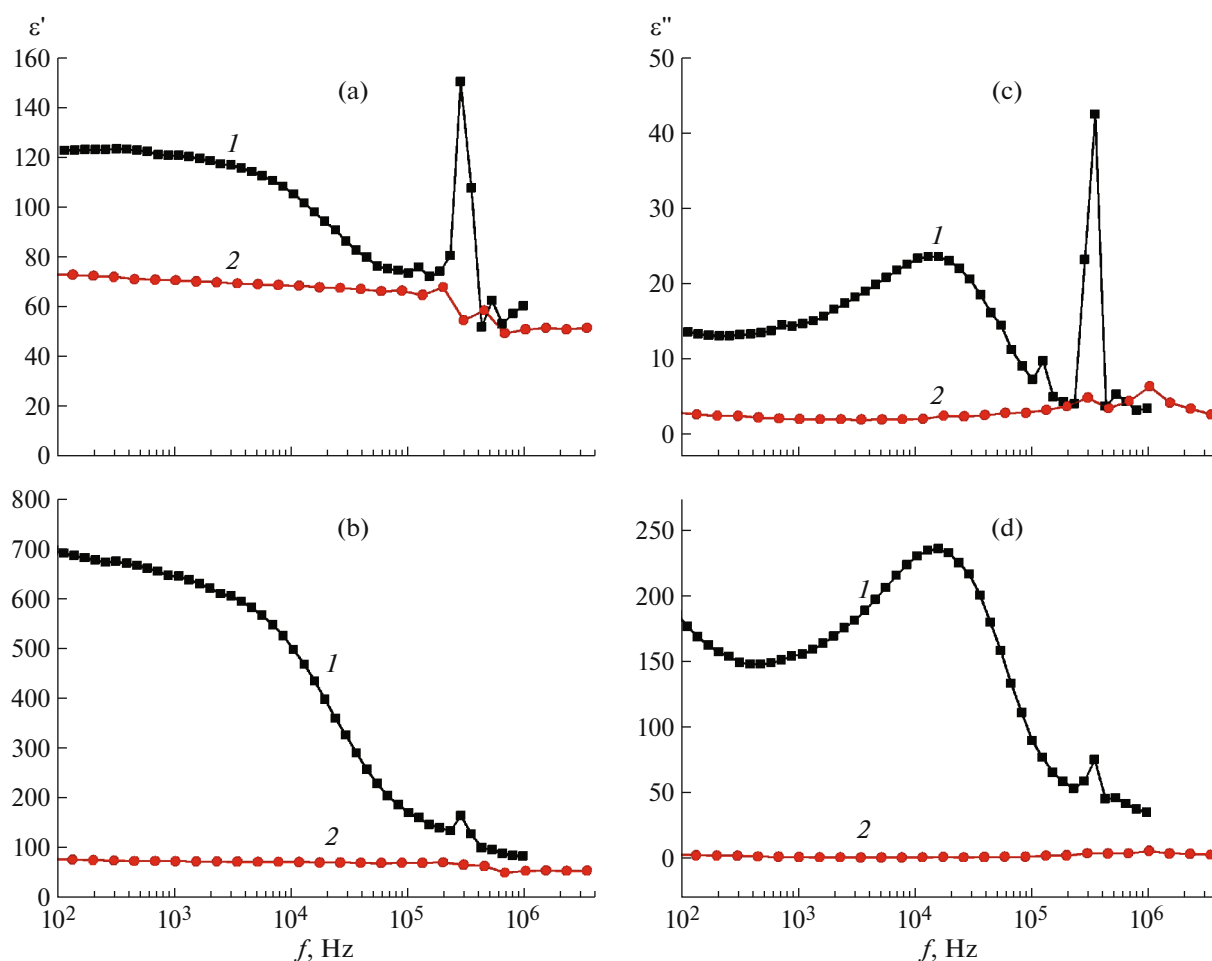


Fig. 2. Dependences $\varepsilon'(f)$ and $\varepsilon''(f)$ for (1) TGS and (2) TGS–TGS + Cr in the (a, c) heating and (b, d) cooling modes at $T = 34^\circ\text{C}$.

cal) temperatures in the heating and cooling modes (Figs. 2, 3). Figure 2 shows the frequency dependences $\varepsilon'(f)$ and $\varepsilon''(f)$ for (1) TGS and (2) TGS–TGS + Cr upon heating (Figs. 2a, 2c) and cooling (Figs. 2b, 2d). They were measured at $T = 34^\circ\text{C}$, when both crystals are in ferroelectric phase. Two dispersions are revealed in the dielectric spectra of TGS. The first is the Debye-type dispersion, which is observed in the frequency range of 10^3 – 10^5 Hz in both measurement modes. The second is an oscillator-type dispersion at a frequency of $\sim 3 \times 10^5$ Hz, which is most pronounced upon heating. The main feature of the dielectric spectra of TGS–TGS + Cr crystals in comparison with TGS is the absence of dielectric dispersion under both heating and cooling conditions. The Debye dispersion is completely suppressed in TGS–TGS + Cr crystals in both measurement modes, and the oscillator-type dispersion, even if present, only in the form of small fluctuations.

Figure 3 shows the dependences $\varepsilon'(f)$ and $\varepsilon''(f)$ measured in the heating mode at $T = 49^\circ\text{C}$ (Figs. 3a, 3b) and at the temperatures corresponding to the maxi-

um of permittivity $\varepsilon'(T)$ in each crystal (Figs. 3c, 3d); these temperatures are $T = 50.5^\circ\text{C}$ for TGS and $T = 50.75^\circ\text{C}$ for TGS–TGS + Cr. At $T = 49^\circ\text{C}$ (Figs. 3a, 3b), the dielectric spectra of both crystals behave practically identically. The Debye-type dispersion is completely absent in them, but there is an oscillator response, which is more pronounced in pure TGS crystal. At the temperatures corresponding to the maximum of permittivity $\varepsilon'(T)$, the spectra of the TGS and TGS–TGS + Cr crystals (Figs. 3c, 3d) coincide within the measurement error, except for the rise at the boundary of the frequency range under study. Since there was no possibility to expand the frequency range, the analysis was limited by a frequency of 10^6 Hz. The spectra measured in the cooling mode for these temperatures are omitted, because the frequency dependences $\varepsilon'(f)$ and $\varepsilon''(f)$ of both crystals behave like the spectra presented in Figs. 2c and 2d, and only their absolute values change.

A comparative analysis of the dielectric spectra of TGS and TGS–TGS + Cr suggests that the main features in the spectra of crystal with a profile chromium

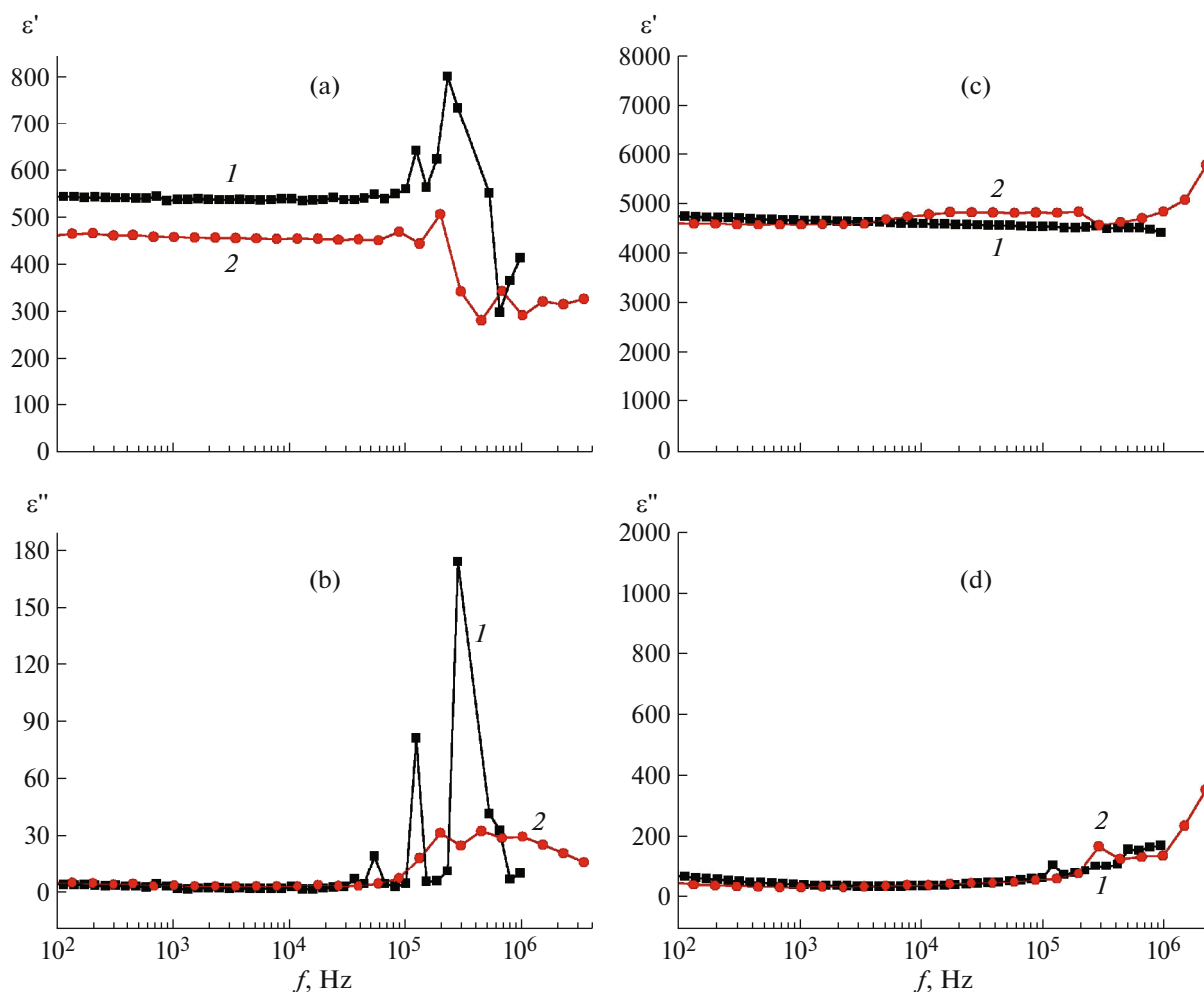


Fig. 3. Dependences $\epsilon'(f)$ and $\epsilon''(f)$ for (1) TGS and (2) TGS–TGS + Cr upon heating: (a, b) $T = 49^\circ\text{C}$ and (c, d) $T = 50.5$ and 50.75°C for TGS and TGS–TGS + Cr, respectively.

distribution are determined by the presence of chromium ions Cr^{3+} and the specificity of crystal growth and distribution of growth defects in these samples. Therefore, we will consider in more detail the specific features of the TGS structure and impurity complexes formed by chromium ions during their incorporation into the lattice. Note that this structure is layered and consists of alternating planes, composed of planar glycines G_2 and G_3 or nonplanar glycines G_1 and SO_4 groups. The planes are spaced by a distance of half the lattice constant ($1/2b$). According to [17, 18] the Cr^{3+} ion is located between the G_2 and G_3 glycines and forms a complex with a coordination number of 6 [19, 20]. A model of the impurity complex of Cr^{3+} with the G_2 , G_3 , and SO_4 groups is presented in Fig. 4. To understand the position of this complex in the unit cell, Fig. 4 shows schematically the projection of the TGS structure on the ab plane (for the symmetry group $2/m$), with indication of possible sites for Cr^{3+} ions between the glycine groups G_2 and G_3 . Impurity

ions can be incorporated into the lattice in only a certain way. Specifically, they can be located along the unit-cell axis b , along which the spontaneous polarization vector is directed when the crystal passes from the paraelectric phase to the ferroelectric phase.

Being an organic compound with a complex structure, TGS has physical and dielectric properties that strongly correlate with the orientational freedom of molecules and molecular groups in the unit cell. Thermal fluctuations in these compounds excite numerous molecular motions and reorientations that are allowed by symmetry. Due to the interaction with the nearest environment, molecules or molecular groups may undergo both almost free rotations and librational motions with a large amplitude or small-angle vibrations around the equilibrium position [21]. Based on this pattern, one can suggest that the suppression of the Debye dispersion observed in the dielectric spectra of TGS–TGS + Cr crystals is most likely related to the presence of impurity complexes, in which the Cr^{3+} ion rigidly connects G_2 and G_3 (Fig. 4) and limits the rota-

tional motion of planar glycines. One can suggest that these complexes determine also the oscillator response in the TGS and TGS–TGS + Cr crystals and, on the whole, their temperature and time dynamics, because molecular groups $G2$ and $G3$ may undergo both rotational and vibrational motion [21].

An important characteristic for estimating the ratio of rotational and vibrational motions caused by the presence of chromium complexes is the chromium ion concentration in the structure.

An X-ray fluorescence analysis of TGS–TGS + Cr samples revealed a periodic character of impurity distribution in the stripes emerging on the (010) surface and showed the chromium concentration to be 0.12–0.14 wt % in TGS + Cr stripes and 0.04–0.06 wt % in TGS stripes [22]. These data make it possible to estimate the average chromium density as approximately one atom per 20 unit cells in impurity stripes. Averaging over the entire sample yields one chromium atom per ~ 50 – 60 unit cells. Despite such a low concentration, the impurity significantly changes the macroscopic characteristics in single-domain regions; a possible reason is the key position of chromium ions along the screw twofold axis (Fig. 4).

Let us consider the periodic structure under study, consisting of alternating stripes 200 μm wide (TGS) and 500 μm wide (TGS + Cr), as a sum of capacitances connected in parallel. One can see that the capacitances composed of TGS + Cr stripes make the main contribution to the dielectric response. The presence of chromium, increasing the unipolarity of crystal, makes it more rigid, which manifests itself in the dielectric spectra of this crystal.

Most of researchers [9–16] relate the relaxation dispersion observed in the range of 1 – 10^6 Hz in the TGS crystals exhibiting domain-wall dynamics to their reversible and irreversible motions. According to the atomic force microscopy data, a fine-grained domain structure is formed in TGS + Cr impurity layers; the domain wall density in this structure exceeds that observed in pure TGS layers by a factor of about 7 [5]. In this case one cannot trace any relationship between the increase in the domain wall density in the impurity stripes of TGS–TGS + Cr crystal and the dielectric dispersion in the frequency range under study

A study of the temperature evolution of dielectric spectra in the frequency range from 10 to 10^7 Hz revealed a characteristic distinction of TGS–TGS + Cr crystals with periodic impurity distribution from TGS [23], specifically: the absence of dielectric dispersion in both heating and cooling modes. This is most likely due to the presence of impurity complexes in the crystal, in which the Cr^{3+} ion rigidly connects $G2$ and $G3$ and limits the rotational motion of planar glycines, and to the peculiar location of these complexes in the lattice, which is related to the periodic

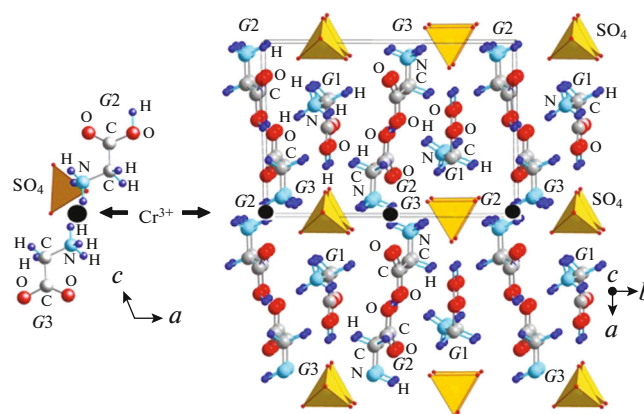


Fig. 4. Model of an impurity complex with $G2$, $G3$, and SO_4 groups, projected onto the ac plane (on the left), and TGS crystal structure with indication of sites of possible location of Cr^{3+} ions between the $G2$ and $G3$ glycine groups, projected onto the ab plane (on the right).

character of impurity distribution in the crystal studied.

CONCLUSIONS

A comparative analysis of the dielectric spectra of nominally pure and impurity crystals plays an important role in the analysis of dielectric dispersion in various ferroelectrics, especially when one can determine the way in which the impurity was incorporated into the lattice. In this case, as our investigation showed, the dielectric spectra can be related to the molecular dynamics of the crystals.

ACKNOWLEDGMENTS

We are grateful to I.F. Kashevich, S.E. Mozzharov, and V.N. Shut for supplying samples of impurity TGS crystals. The experiments were performed using equipment of the Collective-Use Center of Federal Scientific Research Centre “Crystallography and Photonics” of the Russian Academy of Sciences.

FUNDING

This study was supported by the Ministry of Science and Higher Education of the Russian Federation within the State assignment for the Federal Scientific Research Centre “Crystallography and Photonics” of the Russian Academy of Sciences.

REFERENCES

1. S. Hoshino, Y. Okaya, and R. Pepinsky, *Phys. Rev.* **115**, 323 (1959).
2. M. S. Tsedrik, *Physical Properties of Crystals of the Triglycine Sulphate Family in Dependence of Growth Conditions* (Nauka i tekhnika, Minsk, 1986).

3. R. B. Lal and A. K. Batra, *Ferroelectrics* **142**, 51 (1993).
4. V. N. Shut, I. F. Kashevich, and B. E. Votts, *Crystallogr. Rep.* **49** (2), 206 (2004).
5. N. V. Belugina, R. V. Gainutdinov, A. L. Tolstikhina, et al., *Crystallogr. Rep.* **60** (4), 555 (2015).
6. V. Tripadus, A. Radulescu, J. Pieper, et al., *Chem. Phys.* **322**, 323 (2006).
7. S. R. Fletcher, E. T. Keve, and A. C. Skapski, *Ferroelectrics* **14**, 775 (1976).
8. J. M. Hudspeth, D. J. Goossen, T. R. Welberry, and M. J. Gutmann, *J. Mater. Sci.* **48**, 6605 (2013).
9. C. P. Ganea, C. Mindru, and N. Vineticu, *Ferroelectrics* **493**, 165 (2016).
10. A. M. Lotonov, V. K. Novik, and N. D. Gavrilova, *Phys. Solid State* **48** (6), 1171 (2006).
11. V. K. Novik, A. M. Lotonov, and N. D. Gavrilova, *Phys. Solid State* **51** (7), 1414 (2009).
12. H. V. Alexandru, C. Mindru, and C. Berbecaru, *Dig. J. Nanomater. Biostruct.* **7** (3), 1353 (2012).
13. H. V. Alexandru and C. Mindru, *Ferroelectrics* **505**, 216 (2016).
14. J. Zhang, *Phys. Status Solidi A* **193** (2), 347 (2002).
15. J. F. Araújo, J. Mendes Filho, F. E. A. Melo, et al., *Phys. Rev. B* **57** (2), 783 (1998).
16. K. Batra, S. C. Mathur, and A. Mansingh, *Phys. Status Solidi A* **77** (1), 399 (1983).
17. W. Windsch and G. Volkel, *Ferroelectrics* **9**, 187 (1975).
18. S. Wartewig, G. Volkel, and W. Windsch, *Ferroelectrics* **19**, 131 (1978).
19. J. Stankowski, S. Waplak, and V. A. Yurin, *Phys. Status Solidi A* **22** (1), K41 (1974).
20. S. Waplak and A. Ostrovski, *Curr. Top. Biophys.* **33** (Suppl. A), 253 (2010).
21. A. M. Malyarevich and M. R. Posledovich, *Zh. Prikl. Spektrosk.* **63** (6), 1009 (1996).
22. R. V. Gainutdinov, A. L. Tolstikhina, N. V. Belugina, et al., *Crystallogr. Rep.* **63** (5), 784 (2018).
23. G. I. Ovchinnikova, A. P. Eremeev, N. V. Belugina, et al., *Phys. Wave Phenom.* **25** (3), 231 (2017).

Translated by Yu. Sin'kov